Experimental study of dissociative attachment in H_2: Effects of vibrational excitation

O. J. Orient and A. Chutjian
Jet Propulsion Laboratory, California Institute of Technology, Pasadena, California 91109
(Received 15 January 1998; revised manuscript received 22 December 1998)

Dissociative electron attachment (DA) to H_2 has been studied by measuring the outgoing kinetic energies of the $H^-(1s^2)$, with $H(nl)$ in $n=1$ and 2 exit channels. The electron energies E_e studied are 3–16 eV. Effects of vibration-rotation population in H_2 are seen, and the DA results herein are modeled in terms of known cross sections for attachment from $H_2(v'',J'')$. Use is made of magnetically confined electron and ion beams with trochoidal deflection to measure outgoing ion energies. [S1050-2947(99)01506-1]

PACS number(s): 34.80.Gs, 82.80.Fk

I. INTRODUCTION

The study of low-energy electron scattering from molecular H_2 is critical to the understanding of the basic properties of this system, such as resonance phenomena and cross sections [1–7], and potential-energy curves and their asymptotic limits [8–17]. These data are also required to account correctly for the processes active in hydrogen negative-ion discharges [18–21]. For example, the surprising observation of hydrogen-atom wall recombination to produce vibrationally excited H_2 molecules within a hydrogen plasma is relevant to the modeling of these high-brightness ion sources [22–25].

The present work deals with measurements in the dissociative attachment (DA) channels in H_2. By analysis of the kinetic energy of the atomic ionic fragment, one is able to identify the electronic state of the neutral (undetected) atom [26]. Because of the large variation of the DA cross section with the H_2 ground vibrational level [3,9,10,14], one is also able to see clear effects of attachment to molecules which are in excited vibration-rotation levels of the $X\,^1\Sigma_g^+$ ground electronic state. These levels appear to be populated by the mechanism observed earlier, namely dissociation of the H_2 to H atoms by a hot electron-gun filament, followed by wall adsorption, recombination, and release of $H_2(v'',J'')$ into the collision region.

The negative-ion reaction channel studied is DA,

$$e(E_e)+H_2(X\,^1\Sigma_g^+,v''J'')\rightarrow H(nl)+H^-(1s^2). \qquad (1)$$

Here, E_e is the incident electron laboratory energy and $H(nl)$ are all energetically open exit channels for the H atom. Using the methods outlined previously for the $e+NO$ system [26], one is able to identify in Eq. (1) the various open $H(nl)$ channels by measuring the kinetic energy of the outgoing H^- ion.

Details, unique to the present work, of the magnetically confined, trochoidal-analysis system, as well as the kinematics of the DA system, are given in Sec. II. Results are presented and discussed in Sec. III in terms of attachment via the excited $v''J''$ levels, and in terms of the potential-energy curves leading to the $n=1$ and 2 exit channels.

II. EXPERIMENTAL CONSIDERATIONS

A schematic diagram of the apparatus is shown in Fig. 1, and described elsewhere [26,27]. Here, operation with the ions H^+, H^-, and H_2^+ is indicated, although only H^- production and detection is relevant to the present study. The experiment is carried out within a uniform, 6 T magnetic field. Electrons (e) are extracted from a hot, hairpin tungsten filament (F), accelerated to the desired final energy E_e in the range 3–16 eV, and crossed with a beam of H_2 effusing from a 1-mm-diam hypodermic needle. The emerging H^- ions and parent-beam electrons are extracted from the collision region, and deflected in a trochoidal monochromator (TM). No ion extraction potentials were used, and the extraction field arising from contact potentials only is estimated to be less than about 30 V/m. The energy width of the confined electron beam was measured to be 0.4 eV [full width at half maximum (FWHM)]. Use was made of a retarding potential-difference technique with the retarding potential applied to the electron Faraday cup FC_e.

Within TM the faster electrons are deflected only several tenths of a millimeter and are collected in FC_e. The plates of TM are biased symmetrically about the ground potential. The electric field of TM is swept linearly to velocity-analyze the ions. The transmitted ions spiral through two slits and a shielded transmission (TR) cage. TM transmits $m_H=1$ particles, both positively and negatively charged. At the electron

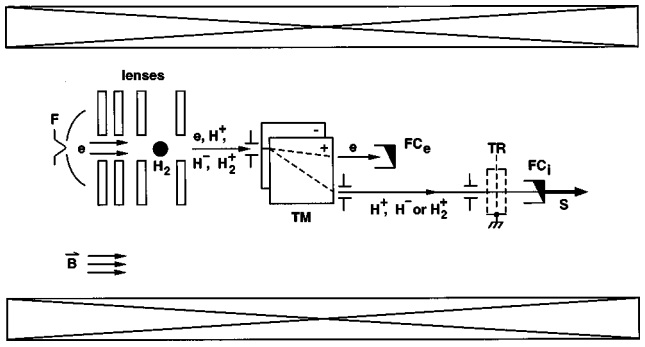

FIG. 1. Schematic diagram (not to scale) of the magnetically confined trochoidal system, shown with capability to produce the several species H^+, H^-, and H_2^+. Electrons (e) from a filament (F) collide with ground-state or vibrationally excited H_2 to form H^- ions by DA. The electron energy range is 3–16 eV. The ions and electrons are separated by the trochoidal monochromator (TM), which also analyzes the different ion velocities as its electric field is swept. The velocity-analyzed ions spiral to the transmission cage TR where the sign of charge (only H^-) is selected by the potential on the central grid. The analog ion signal S is detected at FC_i.

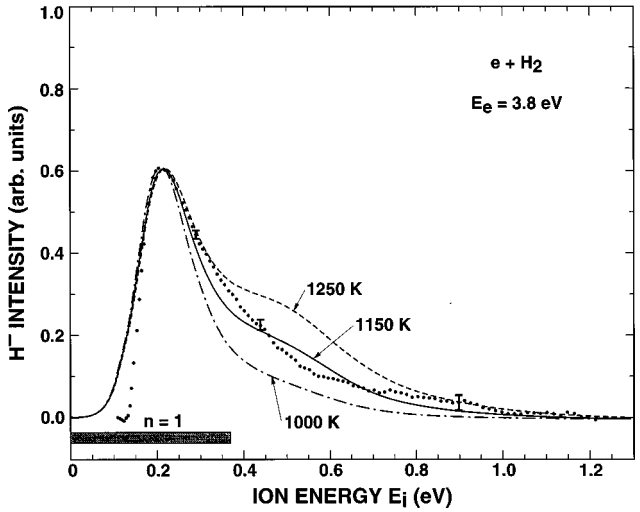

FIG. 2. Dissociative attachment H^- energy spectrum for 3.8 eV incident electron energy. Experimental data are solid points. The spectrum is modeled in terms of a rotation-vibration population at a single indicated temperature T, and DA cross sections from excited $v''J''$ levels [22]. All curves are normalized to the peak of the experimental signal. The shaded interval beneath the peak is the expected peak width in the absence of $v''J''$ excitation ($E^*_{v''J''}=0$), as calculated from Eqs. (2) and (3). Error bars here and elsewhere are statistical, and are shown at the 2σ limit.

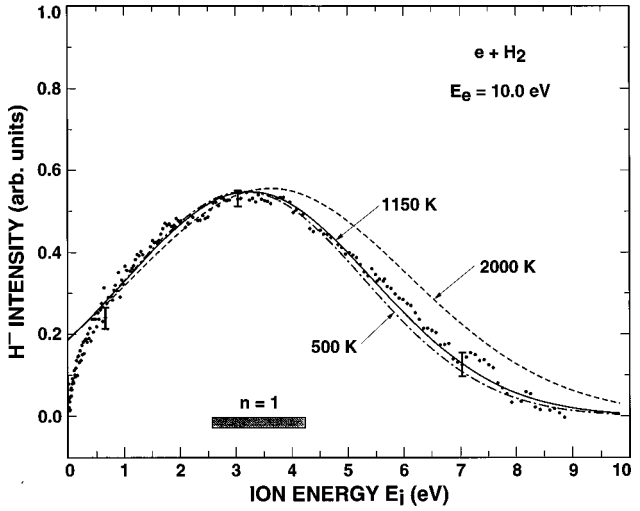

FIG. 3. Same as Fig. 2, but at an incident electron energy of 10.0 eV.

energies used here, only H^- ions are formed [7]. Hence the central grid of TR could be biased +130 V to transmit H^- and reject other positively charged background species. The negative ions are detected in an analog mode in a second ion Faraday cup (FC_i). The ion current S is digitized and stored in a PC. Typical operating pressure near the H_2 beam is 6.5×10^{-5} Pa and at the detector FC_i 6.5×10^{-7} Pa. The electron current ($\approx10^{-7}$ A) and ion current ($\approx10^{-11}$ A) were kept sufficiently low so that space-charge broadening effects in either beam were minimal (electrons) or absent (ions) [27].

III. RESULTS AND DISCUSSION

Ion-energy spectra for the DA process [Eq. (1)] are shown in Figs. 2–4. To understand the energetics of the collision system one treats, as in the O^-/NO study [26], the H and H^- fragments as emerging from a zero center-of-mass (CM) energy. The energy distribution of the outgoing H^- ion is given by [28]

$$E_i=\frac{\mu}{m_{\mathrm{H}}}\Delta E_{\mathrm{CM}}+\cos\theta\left(\frac{4\mu}{M}E_0\Delta E_{\mathrm{CM}}\right)^{1/2}. \qquad (2)$$

Here, E_i is the ion's laboratory energy, m_{H} is the atomic hydrogen mass, μ the reduced mass, and M the total H_2 mass. The angle θ is the CM angle of the outgoing H^- ion relative to the CM velocity along the incident H_2 direction. The initial (thermal) H_2 energy is E_0, and ΔE_{CM} is the total CM energy available to fragment translation. This last quantity is given by

$$\Delta E_{\mathrm{CM}}=[E_e+E^*_{v''J''}-(D_0^0-A+E^*)], \qquad (3)$$

where $E^*_{v''J''}$ is the vibration-rotation energy in the $H_2(X)$ state, D_0^0 the X-state dissociation energy (3.7238 eV), A the electron affinity of H (0.7542 eV), and E^* the energy separation of states H($n=2,3,...$) relative to H($n=1$). The effect of $E^*_{v''J''}$ is to serve as a source of internal energy via vibration and rotation, just as the electron affinity A is an electronic energy source. One may use Eqs. (2) and (3) to calculate the laboratory energies of H^- and compare them to measurements.

Shown in Figs. 2–4 are experimental ion-energy spectra corresponding to the DA process given by Eq. (1). The three electron energies (3.8, 10.0, and 14.3 eV) were selected to correspond to the maxima in negative-ion production [1,2,7]. The attachments at $E_e=3.8$ eV (Fig. 2) and $E_e=10.0$ eV (Fig. 3) are at electron energies below the H($n=2$) threshold so that only a single peak is observed. The excitation at $E_e=14.3$ eV is just above the opening of the H($n=2$) channel. Hence one observes two H^- energy components corresponding to the H atom in an $n=1$ or 2 state. The shaded region under each spectral peak corresponds to the range of labora-

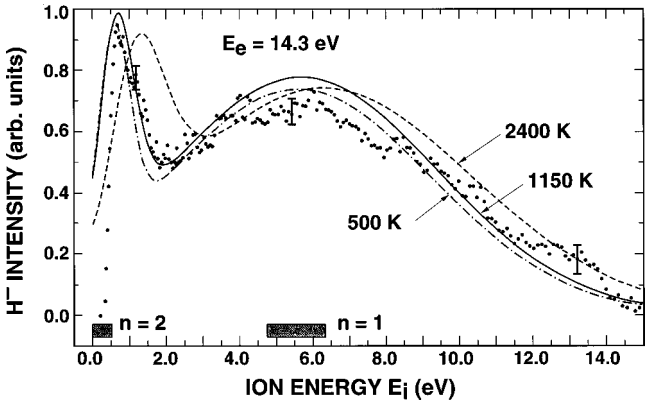

FIG. 4. Dissociative attachment H^- energy spectrum for 14.3 eV incident electron energy. Modeling calculations are as in Fig. 2. The shaded intervals below each peak are the expected peak widths with $E^*_{v''J''}=0$, as calculated for the final atomic states H($n=1$) and H($n=2$).

TABLE I. Energies of H_2 (stated to 0.001 eV) relative to H_2 X $(v''=0, J''=0)$.

Limit	Energy (eV)
$H^-(1s^2)+H(1s)$	3.724
$H(1s)+H(1s)$	4.478
$H^-(1s^2)+H(2l)$	13.922

tory energies given by Eqs. (2) and (3) with θ taken in the entire CM interval $\{0,\pi\}$. An additional small broadening of 0.4 eV (FWHM) due to the measured energy spread of the incident electron beam was also included in the calculated width. The relevant spectroscopic thresholds are listed in Table I.

Identification of the $n=1$ and 2 features was also confirmed by plotting the most probable ion energy E_i against incident electron energy E_e. Results are given in Fig. 5, where the indicated thresholds (Table I) and slope ($\mu/m_H=1/2$) are consistent with reaction (1) and Eq. (2). Also, further spectra were taken at $E_e=3.8$, 10.0, and 14.7 eV, but at *half* the magnetic field intensity ($B=3$ T), hence with half the electric field at TM needed to obtain the same deflection into FC_i. The purpose of these measurements was to test for effects of a larger ion gyroradius, and smaller fringing fields at the entrance and exit of TM. No effects were seen, and the resulting spectra were virtually identical to those shown in Figs. 2–4.

One sees that the peaks in Figs. 2–4 are broader than can be accounted for by Eq. (2) with monochromator broadening, whereas a similar analysis in NO was able to account for the major part of the measured O^- widths [26]. The additional broadening here was presumed to be due to the presence of vibrationally excited H_2 molecules in the target region. While these densities are quite small (as low as 10^{-5} the $v''=0$ population [23,25]), the variation of DA cross section $\sigma_{DA}(v'',J'')$ with v'' is quite steep, increasing by about a factor of 5–10 per vibrational level for the lower levels [3,9,10,14,22,25]. Hence the attachment rate from excited levels—proportional to the product *population* $\times\sigma_{DA}(v'',J'')$—can be comparable to the $v''=0$ rate.

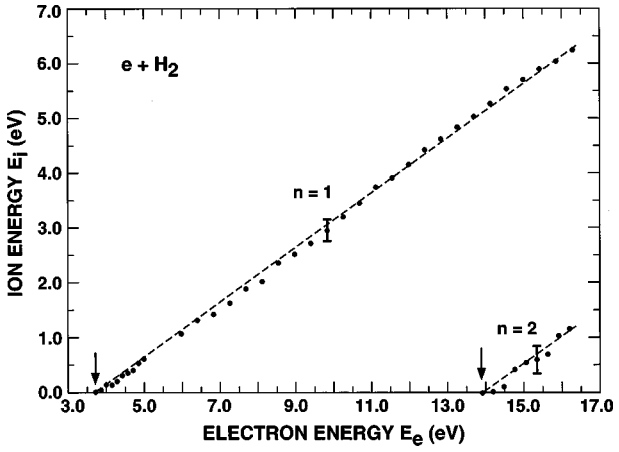

FIG. 5. Energies of the H^- ions at their peak intensities, plotted against electron energy. The straight lines correspond to a kinematic slope of $\mu/m_H=1/2$. Measured threshold energies (arrows) are consistent with those for the opening of the $n=1$ and 2 channels (see Table I).

To model the observed spectra in terms of excited $v''J''$ levels, the Boltzmann vibration-rotation population of H_2 at various vibration-rotation temperatures $T_{v''}, T_{J''}$ was calculated. These populations were then used to weight the $\sigma_{DA}(v'',J'')$. A full set of $\sigma_{DA}(v'',J'')$, calculated using a local complex potential method, was kindly provided by Popović *et al.* [22]. Denoting the excited state and total densities by $N_{v''J''}$ and N, respectively, the relative vibration-rotation population $f_{v''J''}=N_{v''J''}/N$ is given by the standard expression

$$f_{v''J''}=\frac{(2J''+1)\exp-[(E_{v''}/T_{v''}+E_{J''}/T_{J''})/k]}{Q_vQ_J}, \quad (4)$$

where Q_v and Q_J are the vibrational and rotational partition functions, respectively, $E_{v''}$ the vibrational energy (disregarding the zero-point energy, here and in Q_v), $E_{J''}$ the rotational energy, and k the Boltzmann constant. The ion current for each transition can then be expressed as

$$I(E_I)=\mathbb{C}\sum_{v''J''} f_{v''J''}\sigma_{DA}(v'',J'')\exp\frac{-(E_i-E_{v''}-E_{J''})^2 4\ln 2}{W^2}. \quad (5)$$

Here, W is the broadening (full width at half-maximum) due to the resolution of TM [26]. The coefficient $\mathbb{C}$ can be different for each transition, and includes other parameters such as electron current, H_2 gas density, and any electron-neutral spatial overlaps which are not needed for this relative-intensity comparison.

It also includes effects of monochromator beam shear, and differing angular distributions of ions. Full three-dimensional (3D) field-and-trajectories calculations [29] show that the latter effect is more important. That is, high-angle scattering will give a small forward (parallel to $\vec{B}$) velocity component, and those ions will be deflected further in TM. This effect would show up as a tailing of the $n=1$ or 2 peak towards lower ion energies, and cannot be responsible for the higher-energy ions observed in Figs. 2–4. As a check, using the identical experimental geometry, we measured ion-energy spectra for the systems O^-/CO consisting of two transitions, and O^-/O_2 having one transition [29]. Each of these transitions has a symmetry for the intermediate $CO^-(\Sigma^+,\Pi)$ or $O_2^-(\Pi_u,\Sigma_g^+)$ state which allows scattering at 90° [30]. We have obtained very good agreement with previously published ion-energy spectra in both molecules. Results on these additional systems, including the 3D trajectory calculations, will be published separately [29].

One may model the experimental results by assuming a series of $T_{v''}$ and $T_{J''}$ in Eq. (4), then calculating via Eq. (5) the expected signal $I(E_i)$ relative to the peak signal in the experiment. From the first calculations it became clear that the fits were not very sensitive to the separate temperatures, so that all subsequent calculations were carried out using a single temperature $T=T_{v''}=T_{J''}$. The effect of the vibration-rotation energy is to extend the range of possible H^- energies to higher energies. This is clearly seen in Figs. 2–4. One also sees that a single temperature of 1150 K adequately fits the DA results. Previous work had indicated two regimes of relaxation [22,23]. One corresponded to little $v''J''$ relaxation

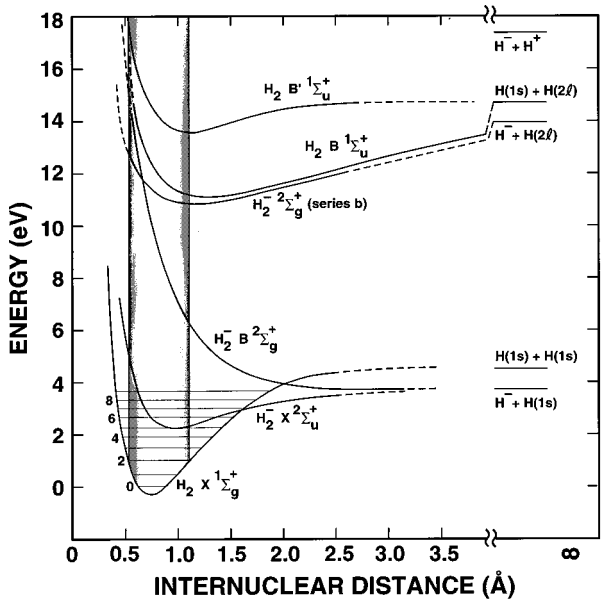

FIG. 6. Partial potential-energy diagram for H_2 showing the relevant electronic states and asymptotic limits. The vertical lines with shading represent edges of the Franck-Condon region, starting from a vibrationally excited level, taken here as $v''=2$.

under conditions of low H_2 pressure. This gave two temperatures $T_{v''}=3000\,\mathrm{K}$ and $T_{J''}=550\,\mathrm{K}$. The second corresponded to $v''J''$ relaxation under conditions of high source pressure or a large number of relaxing collisions, which gave closer temperatures $T_{v''}=1800\,\mathrm{K}$ and $T_{J''}=1500\,\mathrm{K}$. Present results correspond to a higher-relaxed regime, with results $T=T_{v''}=T_{J''}=1150\,\mathrm{K}$. The relaxation is probably due to the fact that vibrationally excited H_2, formed by the sequence of molecular dissociation at the tungsten filament (Fig. 1), followed by surface recombination and ejection, must migrate about 7 cm through the electron-gun lens stack towards TM, after which attachment cannot occur. An estimated average pressure in the stack is 10^{-2} Pa corresponding to a mean free path for H_2-H_2 collisions of 100 cm. Hence the excited H_2 are likely making multiple collisions with the lens walls, rather than with other molecules, to relax to low $v''J''$ populations.

To understand the mechanism for ion production, one must examine the possible potential-energy curves involved. The relevant states of H_2 and H_2^- are given in Fig. 6. A Franck-Condon region is shown within the shaded vertical bars. The observed ion energies can be justified through the intersection of the Franck-Condon region with the potential-energy curves. The DA channel $H^-(1s^2)+H(n=1)$ is accessed through the states $X\,^2\Sigma_u^+$ and $B\,^2\Sigma_g^+$ of H_2^- [8,10,15]. Identification of the state(s) leading to $H^-(1s^2)+H(n=2)$ is more uncertain, but at least one $^2\Sigma_g^+$ state has been identified as responsible for the series *b* resonances, and leads to the appropriate atomic asymptote [11–13]. In terms of angular distributions [30], the first $X\,^1\Sigma_g^+ \rightarrow X\,^2\Sigma_u^+$ transition would give an H^- differential cross section (DCS) peaking at 0°; the $X\,^1\Sigma_g^+ \rightarrow B\,^2\Sigma_g^+$ peaking at 0° and 90°; and the $X\,^1\Sigma_g^+ \rightarrow {}^2\Sigma_g^+$ (series *b*) peaking at 0° and 90°. This agrees with experimental observations reported in at least the first two cases [4]. There do not appear to be experimental DCS's via the higher-energy states leading to the $n=2$ channel. Also, *other* H_2^- states are undoubtedly contributing to this channel but the number, symmetry, and asymptotic limit of these states must await accurate potential-energy calculations in this higher-energy region. Further experimental and theoretical data on the higher-energy H_2^- states would seem to be called for.

ACKNOWLEDGMENTS

We thank C. Schermann for providing us with calculated DA cross sections for $H_2(v'',J)$. We also thank M. R. Darrach and J. B. Greenwood for helpful discussions. This work was carried out at the Jet Propulsion Laboratory, California Institute of Technology, and was supported by the National Science Foundation through agreement with the National Aeronautics and Space Administration.

[1] G. J. Schulz, Phys. Rev. **113**, 816 (1959); G. J. Schulz and R. K. Asundi, *ibid.* **158**, 25 (1967).
[2] D. Rapp, T. E. Sharp, and D. D. Briglia, Phys. Rev. Lett. **14**, 533 (1965).
[3] M. Allan and S. F. Wong, Phys. Rev. Lett. **41**, 1791 (1978).
[4] M. Tronc, F. Fiquet-Fayard, C. Schermann, and R. I. Hall, J. Phys. B **10**, 305 (1977).
[5] K. Köllmann, J. Phys. B **11**, 339 (1978).
[6] M. Landau, R. I. Hall, and F. Pichou, J. Phys. B **14**, 1509 (1981).
[7] S. K. Srivastava and O. J. Orient, in *Production and Neutralization of Negative Ions and Beams*, edited by K. Prelec (AIP, New York, 1984), p. 56.
[8] J. N. Bardsley and J. S. Cohen, J. Phys. B **11**, 3645 (1978).
[9] J. N. Bardsley and J. M. Wadehra, Phys. Rev. A **20**, 1398 (1979).
[10] J. M. Wadehra, in *Nonequilibrium Vibrational Kinetics*, edited by M. Capitelli (Springer, New York, 1986), Chap. 7.
[11] J. Comer and F. H. Read, J. Phys. B **4**, 368 (1971).
[12] A. Huetz and J. Mazeau, J. Phys. B **16**, 2577 (1983).
[13] M. Tronc, R. I. Hall, C. Schermann, and H. S. Taylor, J. Phys. B **12**, L279 (1979).
[14] A. P. Hickman, Phys. Rev. A **43**, 3495 (1991).
[15] T. E. Sharp, At. Data **2**, 119 (1971).
[16] W. A. Chupka, P. M. Dehmer, and W. T. Jivery, J. Chem. Phys. **63**, 3929 (1975).
[17] E. R. Davidson, in *Physical Chemistry, An Advanced Treatise, V. III*, edited by D. Henderson (Academic, New York, 1969), Chap. 3; and private communication.
[18] D. A. Skinner, A. M. Bruneteau, P. Berlemont, C. Courteille, R. Leory, and M. Bacal, Phys. Rev. E **48**, 2122 (1993).
[19] J. R. Hiskes and A. M. Karo, J. Appl. Phys. **67**, 6621 (1990); J. R. Hiskes, Rev. Sci. Instrum. **63**, 2702 (1992).
[20] Yu. Belchenko, Rev. Sci. Instrum. **64**, 1385 (1993).
[21] M. Bacal, C. Michaut, L. I. Elizarov, and F. El Balghiti, Rev. Sci. Instrum. **67**, 1138 (1996).

[22] D. Popović, I. Čadež, M. Landau, F. Pichou, C. Schermann, and R. I. Hall, Meas. Sci. Technol. **1**, 1041 (1990); see also C. Schermann, F. Pichou, M. Landau, I. Čadež, and R. I. Hall, J. Chem. Phys. **101**, 8152 (1994).
[23] R. I. Hall, I. Čadež, M. Landau, F. Pichou, and C. Schermann, Phys. Rev. Lett. **60**, 337 (1988).
[24] I. Čadež, C. Schermann, M. Landau, F. Pichou, D. Popović, and R. I. Hall, Z. Phys. D **26**, 328 (1993).
[25] S. Gough, C. Schermann, F. Pichou, M. Landau, I. Čadež, and R. I. Hall, Astron. Astrophys. **305**, 687 (1996).
[26] O. J. Orient and A. Chutjian, Phys. Rev. Lett. **74**, 5017 (1995).
[27] O. J. Orient, A. Chutjian, K. E. Martus, and E. Murad, Phys. Rev. A **48**, 427 (1993).
[28] F. Brouillard and W. Claeys, in *Physics of Ion-Ion and Electron-Ion Collisions*, edited by F. Brouillard and J. Wm. McGowan (Plenum, New York, 1983), p. 415.
[29] O. J. Orient, M. R. Darrach, and A. Chutjian (unpublished).
[30] G. H. Dunn, Phys. Rev. Lett. **8**, 62 (1962).